SAND87-1694
Unlimited Release
Printed September 1987

Distribution
UC-94E

Calculation of Creep Induced Volume Reduction of the Weeks Island SPR Facility Using 3-D Finite Element Methods

Dale S. Preece
Applied Mechanics Division I
Sandia National Laboratories
Albuquerque, New Mexico 87185

Abstract

Creep induced storage volume reduction has been calculated for the bilevel room and pillar salt mine at the Weeks Island SPR facility where 73 million barrels (MMbbl) of crude oil are currently stored. The calculation was performed using three separate 3-D finite element models which represent the three categories of pillars found in the mine. The idealized pillars in the three categories are all 100 feet square. The first pillar model was 25 feet high with loading representative of the lower level of the mine. The second pillar model was 75 feet high with loading representative of the lower level and the third model was 60 feet high with loading representative of the upper level of the mine. Vertical and horizontal closures measured by Morton Salt over a six-year period are compared with calculated closures and found to be in good agreement. The volume change associated with each of the three pillar models was proportioned according to the mine volume it represents to obtain the total mine volume at each time step. The volume calculation spans the years 1955 to 2012 and indicates that the mine will exhaust its excess storage space in the early 1990's. This will require that several million barrels of oil be withdrawn from the mine during its planned lifetime.

Contents

List of Figures

List of Tables

1. Introduction

The Weeks Island salt dome is located south of New Iberia, Louisiana in the south central part of the state and along the coast. The island, which rises 170 feet above the surrounding marshland, is approximately two miles in diameter. Two site characterization studies have been performed and contain important geotechnical details about the island (Acres International, 1977 and 1987).

Rock salt mining production began in 1902 with a room and pillar mining operation on what is now termed the upper level. The floor of this level is at approximately -535 msl (feet below Mean Sea Level). Mining on the lower level, which has a floor elevation of approximately -735 msl, began in 1955.

The U. S. Department of Energy purchased these two mine levels and the space directly above them for the U. S. Strategic Petroleum Reserve (SPR) program in 1975. The two levels of rooms and pillars were modified for oil storage by constructing bulkheads at all entrances and constructing drawdown pumping facilities and access drifts in the salt above the oil storage area. In late 1979 and early 1980 the facility was filled with 73 million barrels (MMbbl) of crude oil. The two oil storage levels are shown schematically in Figure 1.1.

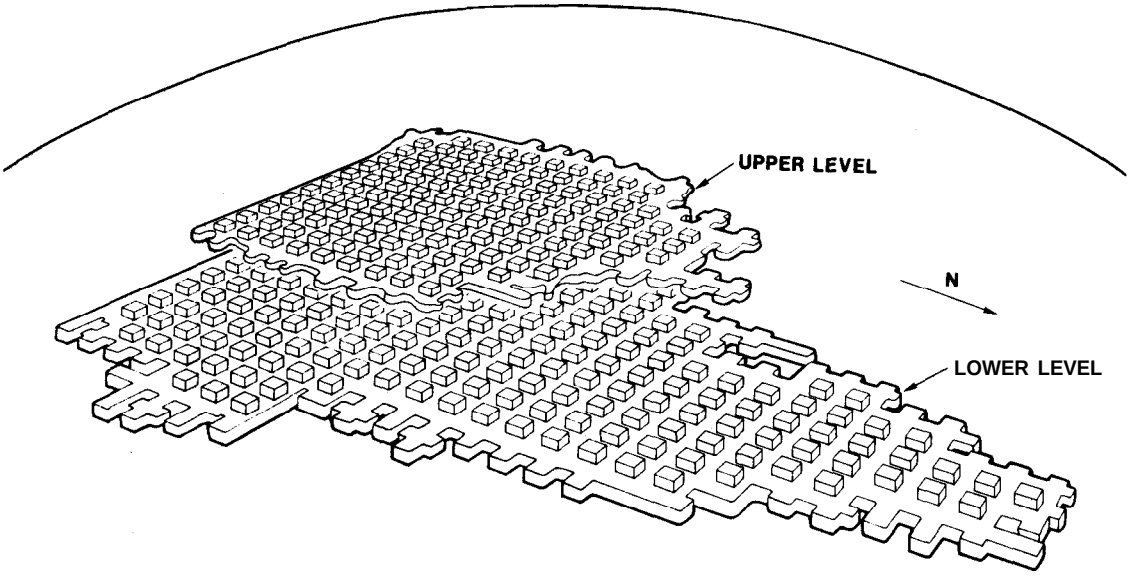

Figure 1.1: Schematic Drawing of the Two SPR levels at Weeks Island

Two-dimensional finite element calculations addressing the structural stability of the two oil storage levels were performed as part of the initial geotechnical investigations (Hilton et al, 1979) (Acres International, 1977). Two-dimensional calculations were also performed to determine the safe spacing between the lower storage level and a proposed Morton mine below the oil storage area (Preece and Krieg, 1984). However, due to the three-dimensional nature of the room and pillar mine and the lack of a three-dimensional computational creep capability, volume loss calculations using finite element methods were not performed until now.

In this study the total mine volume is assumed to be contained by rooms and pillars in three different geometric categories. In all three categories the pillars are assumed to be 100 feet square with 50 foot drifts surrounding each pillar and separating it from adjacent pillars. The first two finite element models assume loading representative of the lower mine level with the first model having a 25 foot high room and the second a 75 foot high room. The third finite element model assumed loading representative of the upper mine level with a 60 foot high room. The volume change of each of the three pillar models was proportioned according to the mine volume it represents to obtain the total mine volume at each time step. The volume calculations span the years 1955 to 2012.

2. Finite Element Computer Programs

JAC3D (Biffle, 1986) is a finite element computer program developed for efficient nonlinear analysis of three-dimensional solids. It employs the conjugate gradient iterative technique to obtain a solution. Spatial integration is performed using a single Gauss point in each eight node hexahedral element. An hourglass viscosity technique is used to control the zero energy modes that occur with single point integration. The single point integration combined with the explicit nature of the program and exploitation of CRAY-XMP computer architecture results in very efficient execution. This has made 3-D creep analyses possible on real configurations. Several examples of previous 3-D creep calculations performed with this program are documented in Preece and Sutherland, 1986; Preece, 1986 and Arguello, Munson and Preece, 1987.

The implementation of the secondary creep formulation is described by Krieg, 1983. This creep formulation is not restricted to JAC and JAC3D but has been used in other finite element programs (Stone et al, 1985).

3. Material Properties For Rock Salt

Salt core from Weeks Island has been tested quasi-statically for strength and elastic constants (Hansen, 1977) but documentation of any creep tests has not been found. Even though creep properties vary from site to site it has been shown that the variance from one site to another is usually within the data scatter at any particular site (Herrmann and Lauson, 1981). Thus, the creep model parameters derived from extensive triaxial creep testing of West Hackberry salt have been used in this study (Wawersik and Zeuch, 1984). The secondary creep model is implemented in the finite element program by expressing the creep strain rate magnitude, $\dot{\bar{e}}$, as a function of effective stress, $\bar{\sigma}$

$$\dot{\bar{e}} = D exp(\frac{-Q}{RT})\bar{\sigma}^{n} \qquad (3.1)$$

where D and n are constants and Q is an activation energy $(\frac{cal}{mole})$, R is the universal gas constant (1.987 $\frac{cal}{mole\ K}$) and T is the material temperature (K). The laboratory determined creep coefficients for West Hackberry salt are given in Table 3.1 along with the elastic constants.

Table 3.1: West Hackberry Secondary Creep Formulation

D = 1.45E-30 $\frac{1}{(day)(psf)^n}$	
Q = 12.0 $\frac{kcal}{mole}$	
n = 4.73	
Young's Modulus = 5.1E7 psf	0.354 X 10^6 psi
Poisson's Ratio = 0.30	

The magnitude of the creep strain rate, $\dot{\bar{e}}$, and the effective stress, $\bar{\sigma}$, can be calculated from the creep strain rate tensor, $\dot{e}^c$, and the deviatoric stress tensor, σ',

respectively as follows.

$$\dot{\bar{e}} = \sqrt{\frac{2}{3}\dot{e}^c\dot{e}^c} \tag{3.2}$$

$$\bar{\sigma} = \sqrt{\frac{3}{2}\sigma'\sigma'} \tag{3.3}$$

The flow rule relating the creep strain rate tensor is related to the deviatoric stress tensor by

$$\dot{e}^c = |\dot{e}^c|\frac{\sigma'}{|\sigma'|} \tag{3.4}$$

The components of the total strain rate tensor, $\dot{e}_{ij}$, are obtained by summing the components of creep strain rate tensor, $\dot{e}^c_{ij}$, along with the components of the bulk, elastic and thermal strain rate tensors as follows.

$$\dot{e}_{ij} = \dot{e}^c_{ij} + \frac{\nu}{E}\dot{\sigma}_{kk}\delta_{ij} + \frac{1+\nu}{E}\dot{\sigma}_{ij} + \alpha\dot{T}\delta_{ij} \tag{3.5}$$

Where σ_{ij} are the components of the stress tensor, ν is Poisson's ratio, E is Young's modulus, T is absolute temperature, α is the coefficient of linear thermal expansion, δ_{ij} is the Kronecker Delta. A constant temperature of 300K was assumed for these calculations.

A few references documenting finite element calculations that have employed this secondary creep formulation are: (Krieg et al, 1981), (Branstetter and Preece, 1983), (Preece and Wawersik, 1984), (Morgan et al, 1985) and (Morgan et al, 1986).

The above constitutive model includes only secondary creep which is one of the simplest creep models and has some limitations. The same formulation with the same parameters was used to calculate the closure of the South Drift of the WIPP. Calculated South Drift closures underpredicted measured closures by a factor of approximately three (Morgan et al, 1985 and 1986). For WIPP excavations dividing Young's modulus by 12.5 was found to be a simple, but not necessarily physically meaningful, method for bringing the calculated closures into agreement with measured closures (Morgan et al, 1987). The same simple method has been applied in this study and the Young's modulus shown in Table 3.1 is the measured value for Weeks Island Salt divided by 12.5.

$\frac{6.325\times10^6}{12.5} = \frac{4.4271\times10^6\ \text{psi}}{12.5} = 0.354\times10^6\ \text{psi}$

4. Finite Element Models

4.1 Morton Mining Methods

The geometry of the three finite element models is a direct result of the mining methods used by Morton to create the two oil-filled levels. Figure **4.1** shows a schematic of the mining methods used to develop the mine.

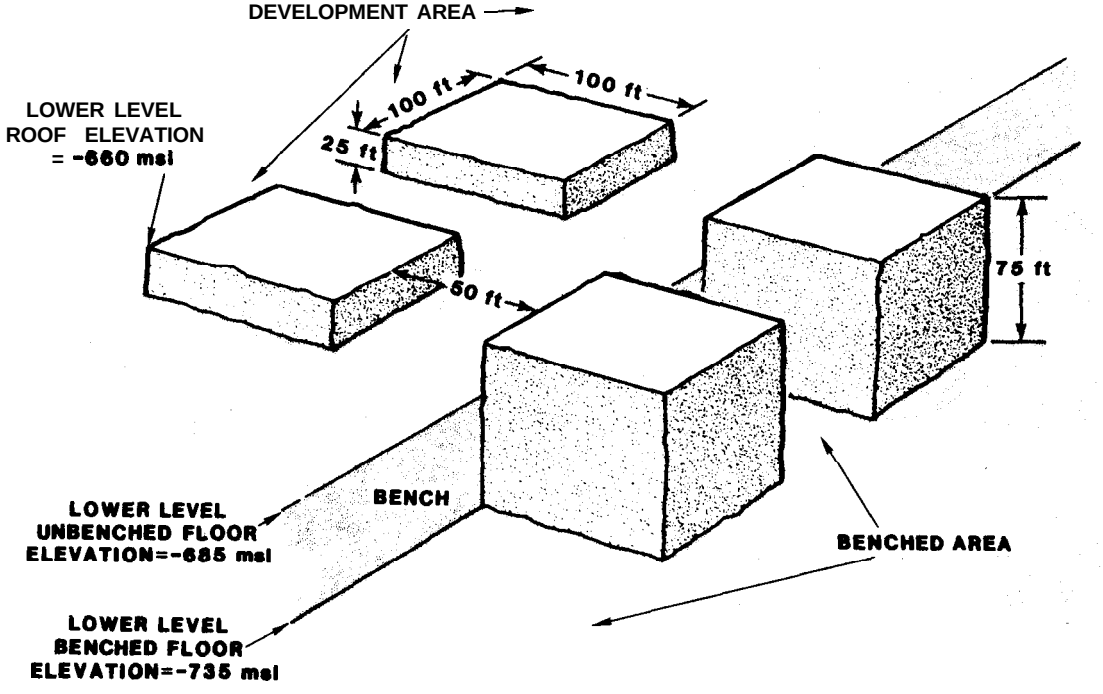

Figure **4.1:** Illustration of Morton Mining Methods by Benching

The first step was to mine the development area which consisted of **100** foot square pillars and rooms that are **50** feet wide and **25** feet high (the width of the rooms on the lower level increased to **70** feet as mining progressed to the northeast and out from under the upper level). The final benched area was created by removing an additional **50** feet of salt from the floor while keeping the pillars at the same spacing and leaving the roof alone. The drifts used for equipment storage and general access to the active mining areas were left unbenched **(25** feet high).

4.2 Idealization of Oil Storage Area Into Three Pillar Categories

The Morton mining methods left four categories of pillars which are: 1) upper level benched, 2) upper level unbenched, 3) lower level benched and 4) lower level unbenched. Table 4.1 shows the division of the mine volume into the four categories (Chabannes, 1987). Since the amount of volume represented by the upper level unbenched category was so small, this category was not represented by a finite element model.

Table 4.1: Distribution of Mine Volume into Pillar Categories

Pillar Category	Volume of Mine Represented (MMbbl)
Upper Level Benched	26.4
Upper Level Unbenched	1.1
Lower Level Benched	38.3
Lower Level Unbenched	10.8
Total	76.6

4.3 Symmetry Planes, Displacement and Pressure Boundary Conditions

An idealized top view of the rooms and pillars is shown in Figure 4.2. It is apparent that there are many planes of symmetry associated with this type of geometry which allows capturing the behavior of the entire array with a much smaller model, provided that the proper boundary conditions are assumed. Only that portion of the array shown in Figure 4.2 was represented in the three finite element models used to treat the three pillar categories.

The finite element model representing the lower level unbenched area is shown in Figure 4.3. This model has 3028 nodal points and 2336 3-D finite elements. The symmetry boundary conditions on the model constrain perpendicular displacements

Table 4.2: Parameters Used to Define Lithostatic Stress

Unit Wt. of Sand and Gravel = 117 $\frac{lb}{ft^3}$ Unit wt of Salt = 135 $\frac{lb}{ft^3}$			
Model	Surface (Elev.)	Top of Salt (Elev.)	Top of Model (Elev.)
Lower Level 25 ft.	+95.0	-70.0	-590.0
Lower Level 75 ft.	+91.0	-70.0	-590.0
Upper level 60 ft.	+80.0	-70.0	-405.0

but allow parallel displacements on each vertical face and the bottom. Lithostatic pressure (isotropic stress state) is applied to the top of the model and gravity induced body forces are applied to the model. In addition, the initial stress state of the model is set to lithostatic. The salt dome has no caprock but is overlaid by a layer of sand and gravel of variable thickness. Table 4.2 contains the unit weights of the materials and the elevations of the material interfaces assumed for calculating the lithostatic stresses associated with each model (Acres International, 1987).

The pressure on the roof and floor of the room and the pillar walls is assumed to be atmospheric from 1955 until 1979. Oil was placed in the mine in 1979 and the pressure is assumed to have increased to oil head pressure. Table 4.3 shows the assumed upper level of the oil in the mine and the elevations of the areas where oil pressure was applied.

The finite element model representing the lower level benched area (75 feet high) is shown in Figure 4.4. This 3-D model has 3838 nodal points and 2976 elements. The boundary conditions are the same as those discussed previously for the 25 foot high model. The finite element model representing the upper level benched area is shown in Figure 4.5. This model has 3595 nodal points and 2784 elements. The boundary conditions are the same as those discussed for the 25 foot high lower level model.

Table 4.3: Parameters Used to Define Oil Pressure

Elevation of Oil/Air Interface = -470 msl

Unit Wt. of oil = 57.4 $\frac{lb}{ft^3}$

Model	Region	Avg. Elev. (msl)	Oil Pressure $(\frac{lb}{ft^2})$
Lower Level 25 ft.	Roof	-660.0	10906.0
	Walls	-672.5	11623.5
	Floor	-685.0	12341.0
Lower Level 75 ft.	Roof	-660.0	10906.0
	Upper 1/3	-672.5	11623.5
	Middle 1/3	-697.5	13058.5
	Lower 1/3	-722.5	14493.5
	Floor	-672.5	11623.5
Upper level 60 ft.	Roof	-475.0	0.0
	Upper 1/3	-485.0	861.0
	Middle 1/3	-505.0	2009.0
	Lower 1/3	-525.0	3157.0
	Floor	-535.0	3731.0

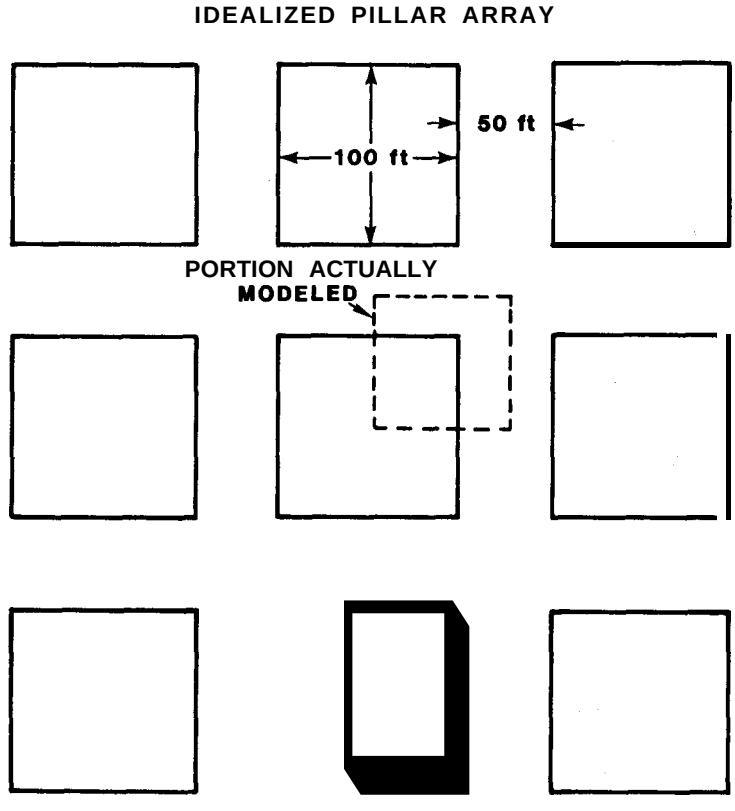

Figure 4.2: Idealized Plan View Showing Portion Modeled

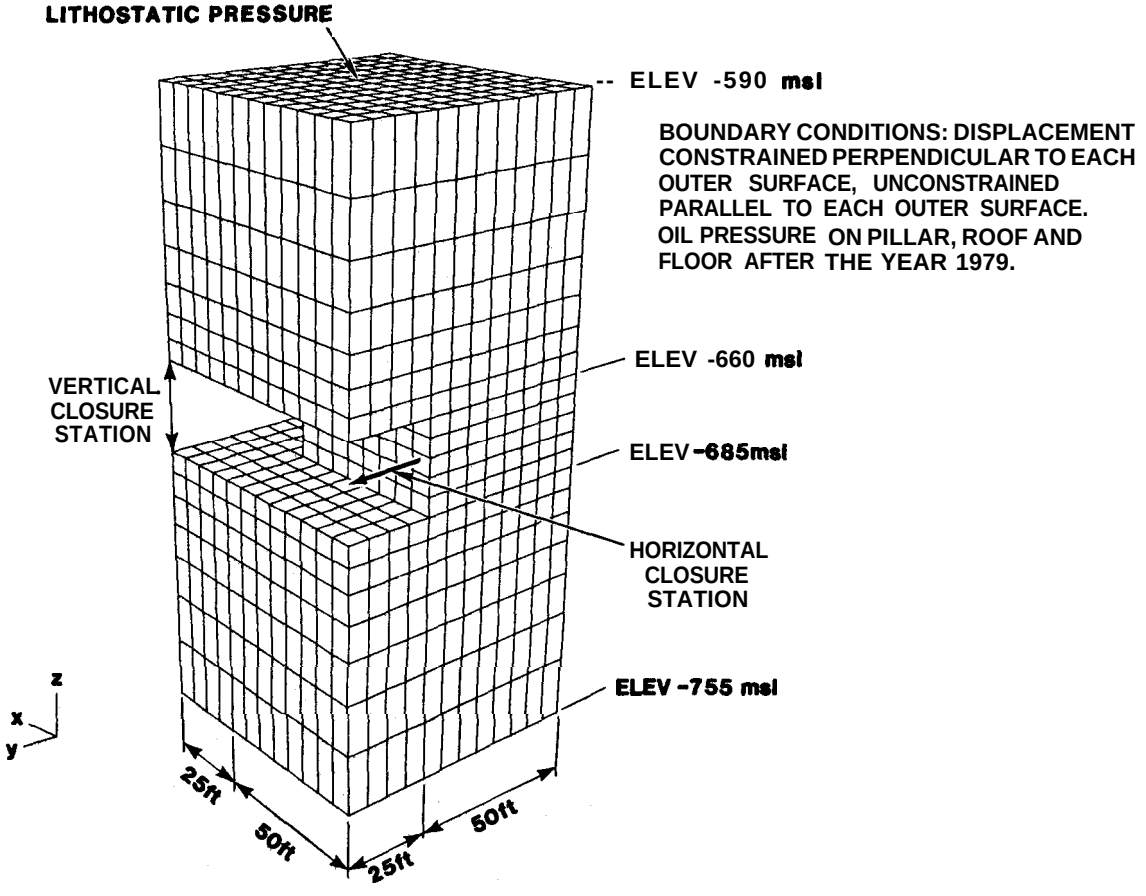

Figure **4.3:** Finite Element Model of **25** Foot High Room on Lower Level

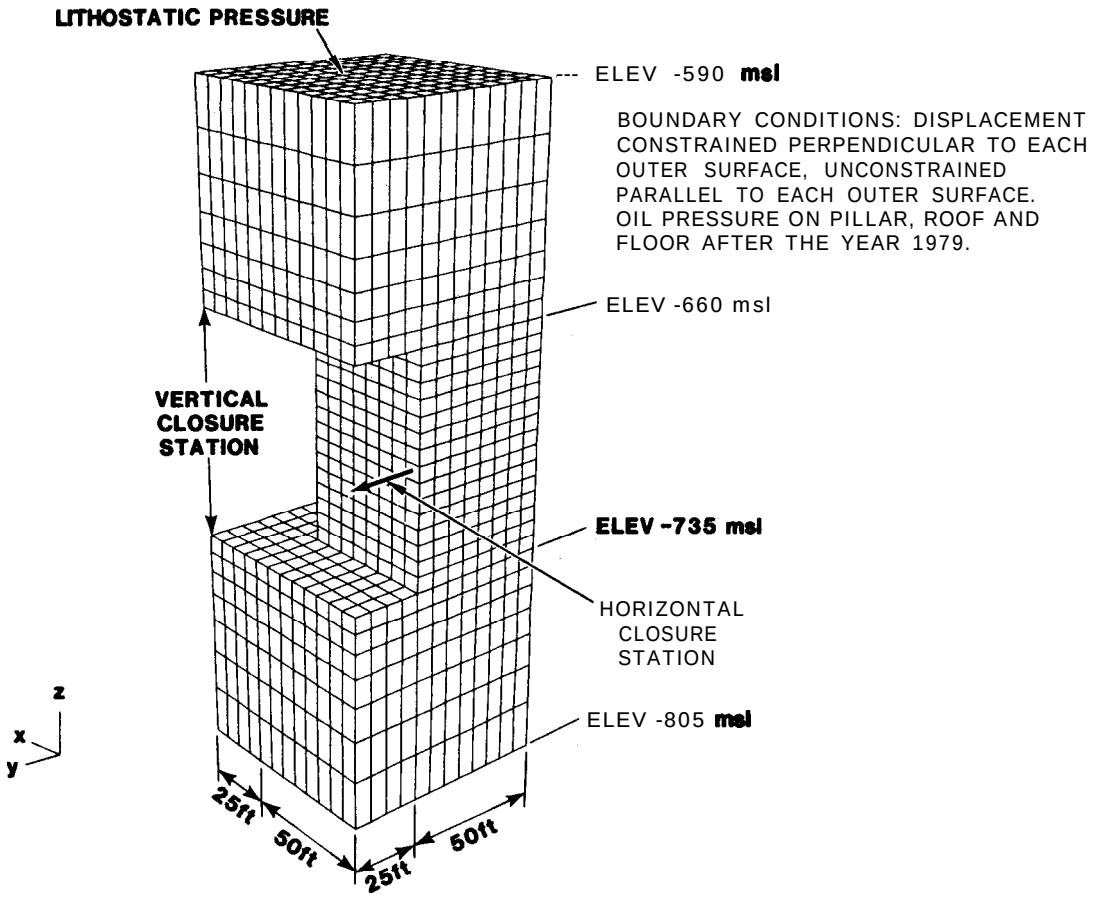

Figure 4.4: Finite Element Model of 75 Foot Room on Lower Level

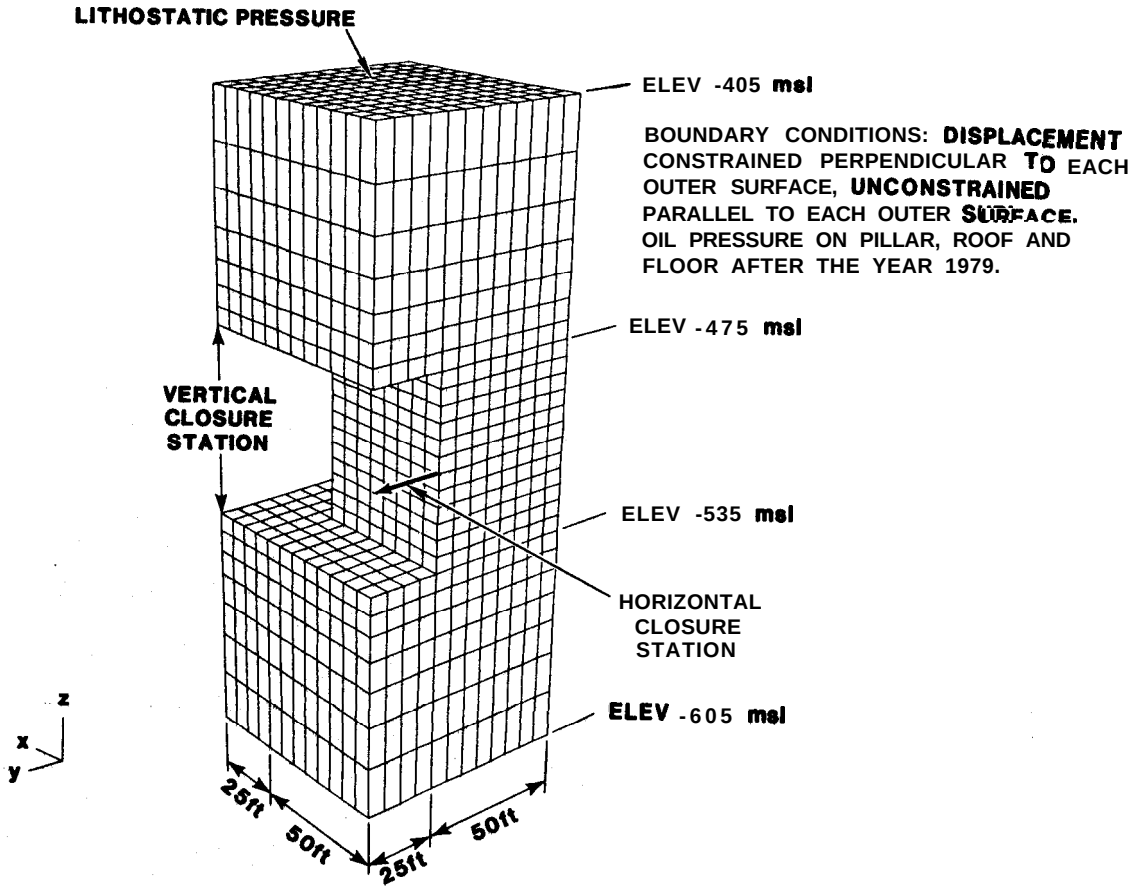

Figure 4.5: Finite Element Model of 60 Foot Room on Upper Level

5. Calculation Results

5.1 Closure and Closure Rates

Figure 4.3 shows the location on the model of the stations where vertical and horizontal closures were calculated. Morton Salt Company established several stations for measuring closure of the mine. As can best be determined, Station 6 was located on the lower level in drift 1 between drifts E and F (Chabannes, 1987) which is an unbenched area on the west boundary of the mine. The exact location and consequently the exact geometry is difficult to determine but it appears to be similar to the geometry of the finite element model. The vertical closure of the finite element model was calculated by summing the absolute value of the displacements of the nodes on the roof and floor. The horizontal closure was calculated by doubling the perpendicular displacement at the center of the wall. Figure 5.1 shows both calculated and measured vertical and horizontal closures. The measured curves start at zero displacement because that is where the gauges were initially set. However, it should be pointed out that some unknown amount of displacement took place before the gauges were installed. The calculated and measured closure curves track each other quite closely over the limited time that the two coexist. Figure 5.2 shows the closure rates determined by numerically differentiating the curves in Figure 5.1. The fact that the measured and calculated closures and closure rates are similar to each other gives some confidence in these calculations.

The calculated closures and closure rates of the lower level 75 foot rooms are shown in Figures 5.3 and 5.4, respectively, and the calculated closures and closure rates of the upper level 60 foot rooms are shown in Figures 5.5 and 5.6, respectively. A comparison of the vertical closure rate of the three different models is given in Figure 5.7. The lower level 75 foot room shows a significantly higher closure rate than the 25 foot lower level room. The relationship between the two is obviously not linear since the height differs by a factor of 3 and the closure rate differs by as much as an order of magnitude. As would be expected from the nonlinear relationship between effective strese and strain rate (Eqn. 3.1), there is also a nonlinear relationship between depth and closure rate. This is seen by comparing the upper level 60 foot room with the lower level 75 foot room where the room height is not significantly different but the closure rate is. The difference can be attributed mostly to a difference in depth.

It is interesting to note the impact that oil fill in 1980 has on the three curves. The closure of the upper level is less effected by oil fill because the oil/air interface

is just below the roof of the upper level. This results in much smaller oil pressures on the walls and floor of the upper level than on the lower level.

5.2 Volume Calculation

The displacements of the roof and floor of the room and the walls of the pillar are processed to determine volume change using the displacement hexahedron method. A brief description of the method will be given here for completeness, however, a more detailed discussion of this method as well as the computer program can be found in Preece and Sutherland, 1986. The first step in the displacement hexahedron method is to determine the element faces on the surface. This is done using the pressure boundary condition information. After each face is identified, a hexahedron is created using the four nodes on the face and four new nodes created at the tips of the four displacement vectors as shown in Figure 5.8. The volume changes of all the displacement hexahedrons on the pressure surface are summed to obtain the total volume change for the model. This operation is carried out at each time step to obtain a data set containing volume change versus time. The validity and accuracy of the method have been shown by Preece and Sutherland, 1986.

The volume of each of the three pillar models was divided into the mine volume represented by that pillar to obtain the number of pillars in each of the three categories. This is summarized in Table 5.1.

Table 5.1: Determination of Number of Pillars in Each Category

Model	Volume/Pillar	Volume Represented	No. of Pillars
60 ft. Upper Level	0.133571	26.4	197.65
75 ft. Lower Level	0.166963	38.3	229.39
25 ft. Lower Level	0.055654	10.8	194.69

Note: Volume units are MMbbl

A check on the number of pillars was made by counting the pillars on the survey maps (Acres International, 1987) of the mine. A count of the benched pillars on the lower level shows approximately 215 which compares well with the calculated value of 229.39. A count of the lower level unbenched pillars shows approximately 120 pillars which is considerably below the calculated value of 194.69. The reason for the discrepancy is that much of the volume in the unbenched areas is contained in drifts around the outer margin of the mine. These unbenched drifts have solid salt on one side and benched 75 foot pillars on the other side. These unbenched drifts are accounted for in this study by lumping them with the unbenched pillars. A count of the number of pillars on the upper level shows approximately 130 pillars. This count also does not include the margin around the outside which probably accounts for most of the discrepancy between the counted number of 130 and 197.65 from Table 5.1 which was calculated using the ratio between pillar model volume and total benched upper level volume.

Figure 5.9 shows the volume reduction $(\triangle V)$ versus time obtained by multiplying the volume change of each model by the number of pillars (Table 5.1) in that category. As expected the lower level 75 foot rooms experience the most volume reduction and dominate the total response. Oil fill in 1980 also has a more significant impact on the volume reduction curve for the lower level 75 foot rooms. The total volume $(V_o - \mathrm{AV})$ versus year curve in Figure 5.10 was developed by assuming that the mine had a survey volume $(V_o)$of 76.6 MMbbl in 1977 (Fenix & Scisson, 1978). Thus, the initial mine volume shown in 1955 was adjusted so that the volume reduction between 1955 and 1977 gave a 1977 volume of 76.6 MMbbl. The portion of the curve before 1975 does not mean much since the mine was in the process of being created and the volume did not exist. From 1975 onward the curve is realistic since mining stopped at that time and the mine was in a state similar to what is represented by the three finite element models.

It is interesting to note that, according to this model, the mine lost approximately one MMbbl between the time the survey was completed in 1977 and the time mine fill began in 1980. This may help explain the discrepancies experienced between the measured strapping curve (oil/air interface level versus volume) and the strapping curve produced from the mine survey (Fenix & Scisson, 1978).

The curve in Figure 5.10 shows that the storage volume is decreasing and in the early 1990's will approach 74 MMbbl. Since the amount currently stored is approximately 73 MMbbl this will leave only one MMbbl of excess space which probably isn't sufficient. The curve in Figure 5.10 was numerically differentiated to obtain the volume change rate curve shown in Figure 5.11. This curve gives a volume change rate of 154,000 bbl/year in 1987. This compares well with 165,000 bbl/year, the approximate volume change rate calculated from the measured movement of the oil/air

interface (Chabannes, 1987). This correlation of model to field data gives some confidence in using this model to extrapolate into the future.

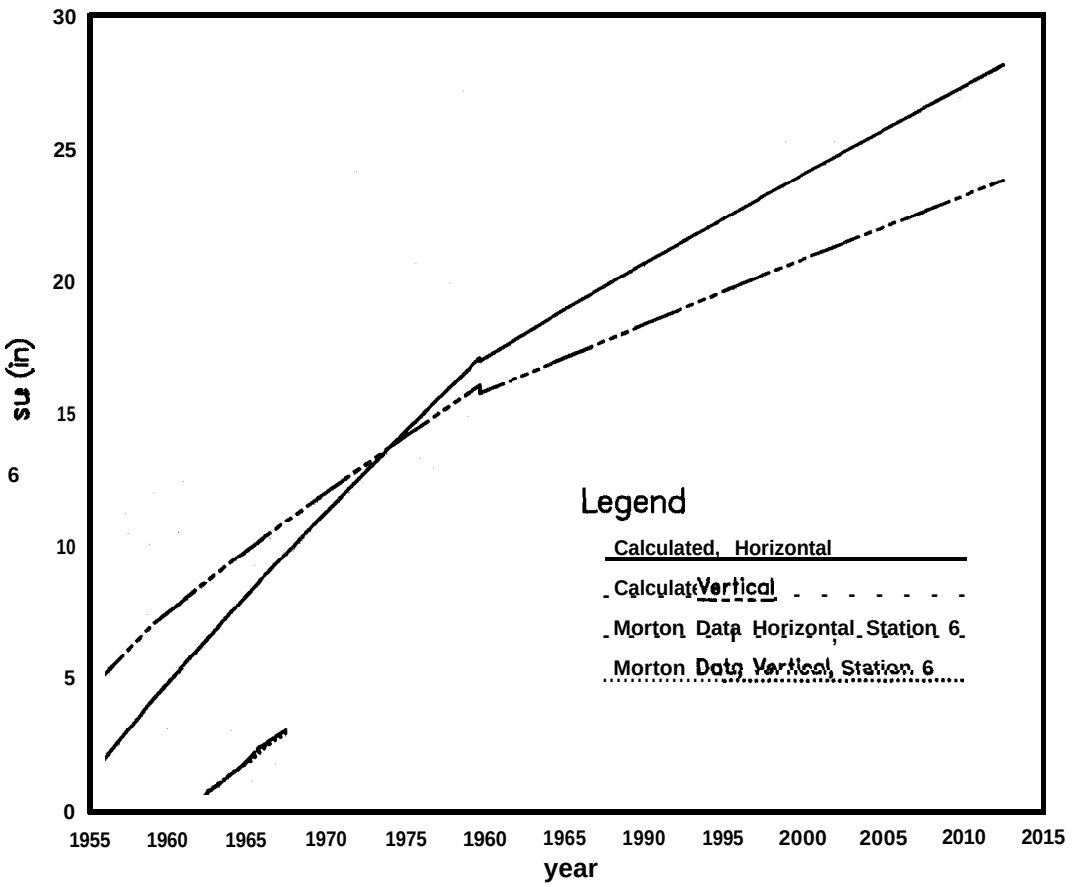

Figure 5.1: Horizontal and Vertical Closure of 25 Foot Room With Morton Data

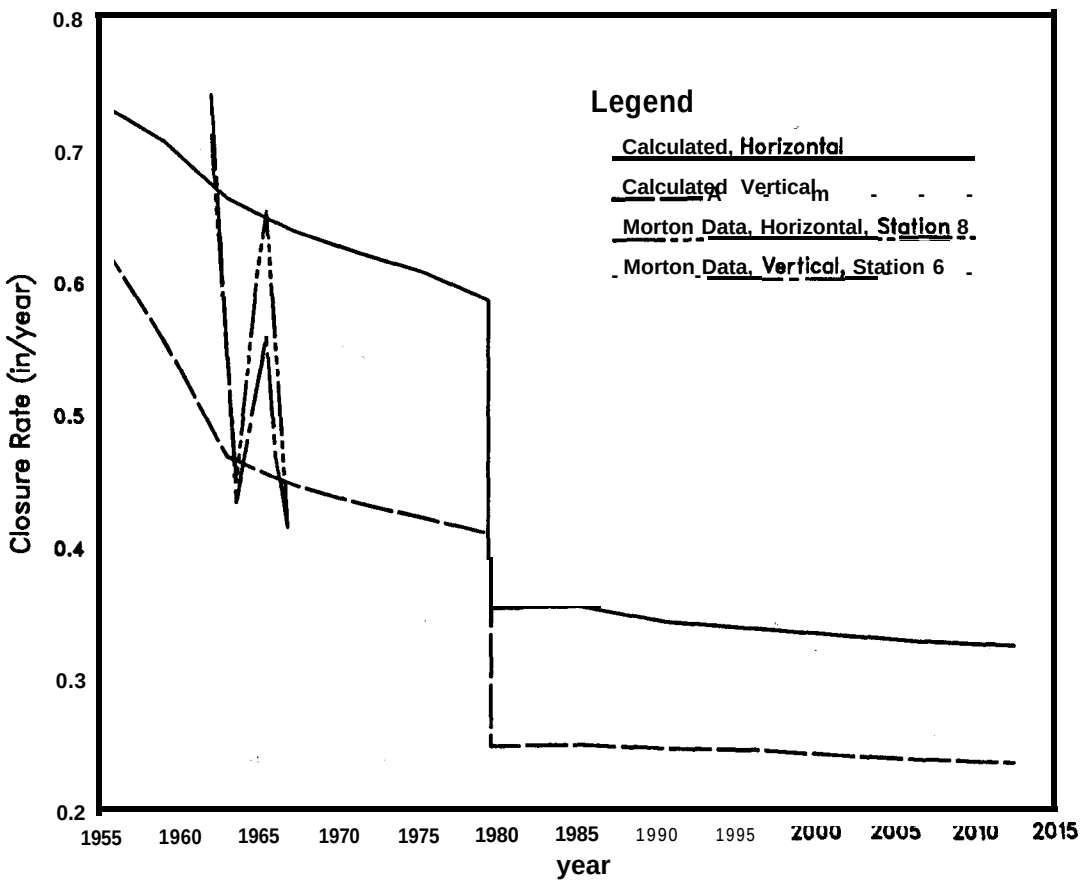

Figure 5.2: Horizontal and Vertical Closure Rate of 75 Foot Room With Morton Data

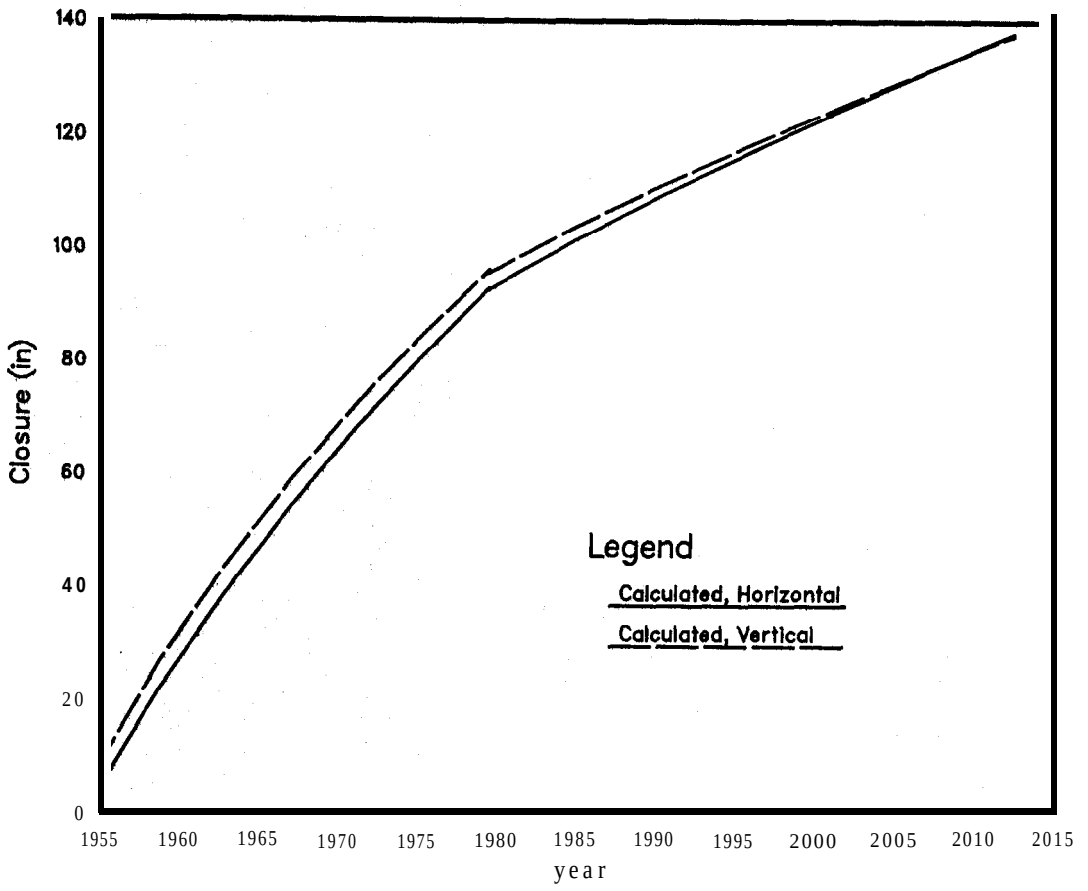

Figure 5.3: Horizontal and Vertical Closure of 75 Foot Room

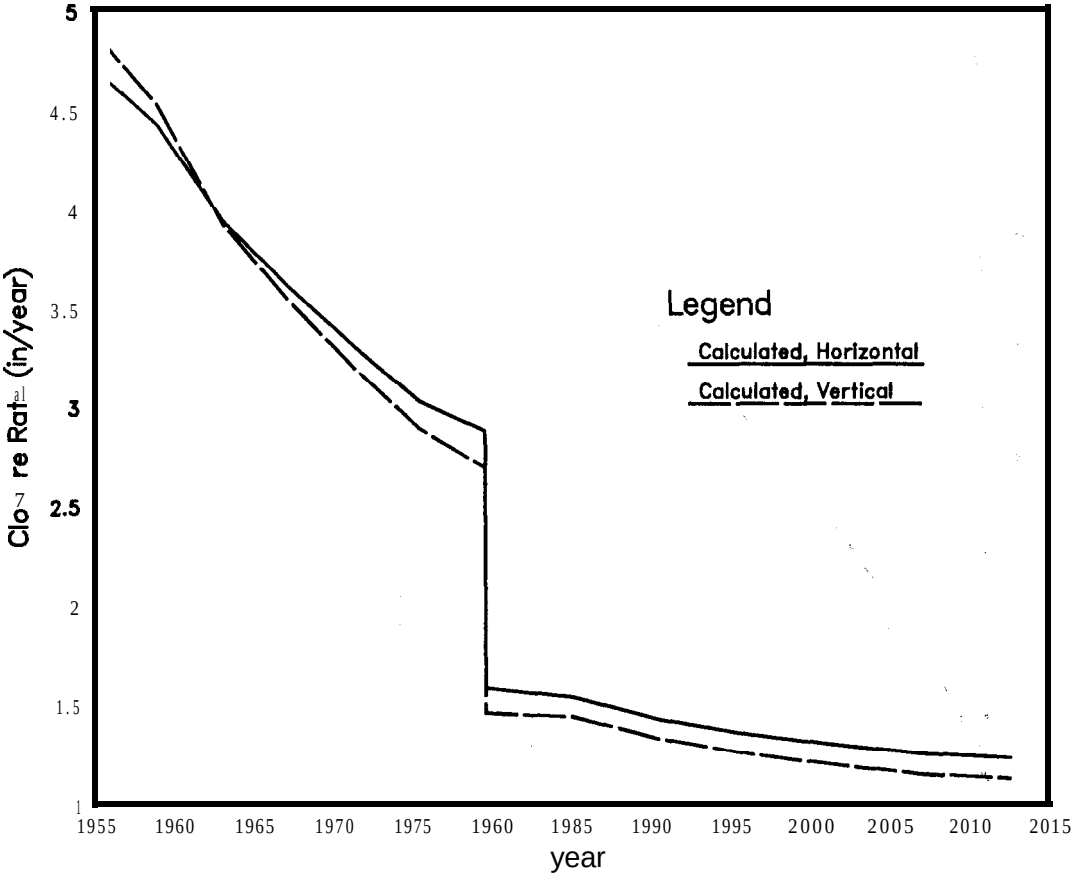

Figure 5.4: Horizontal and Vertical Closure Rate of 75 Foot Room

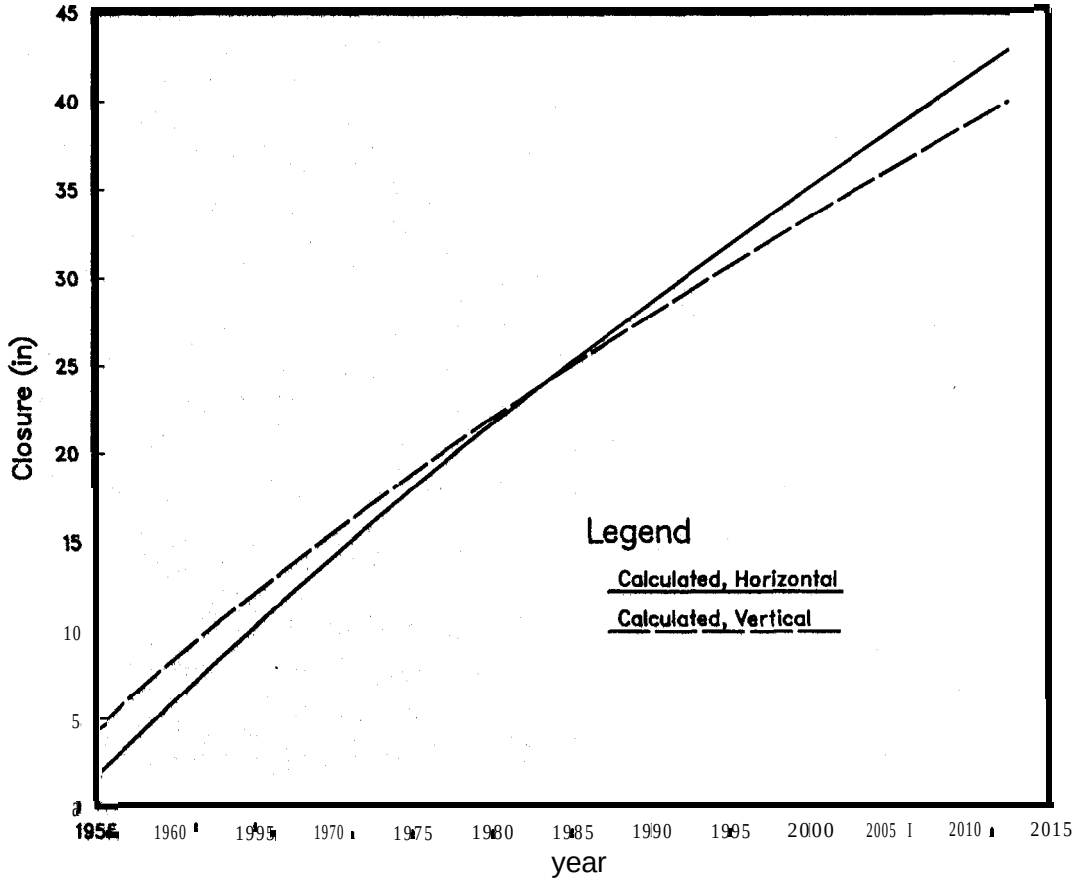

Figure 5.5: Horizontal and Vertical Closure of 60 Foot Room

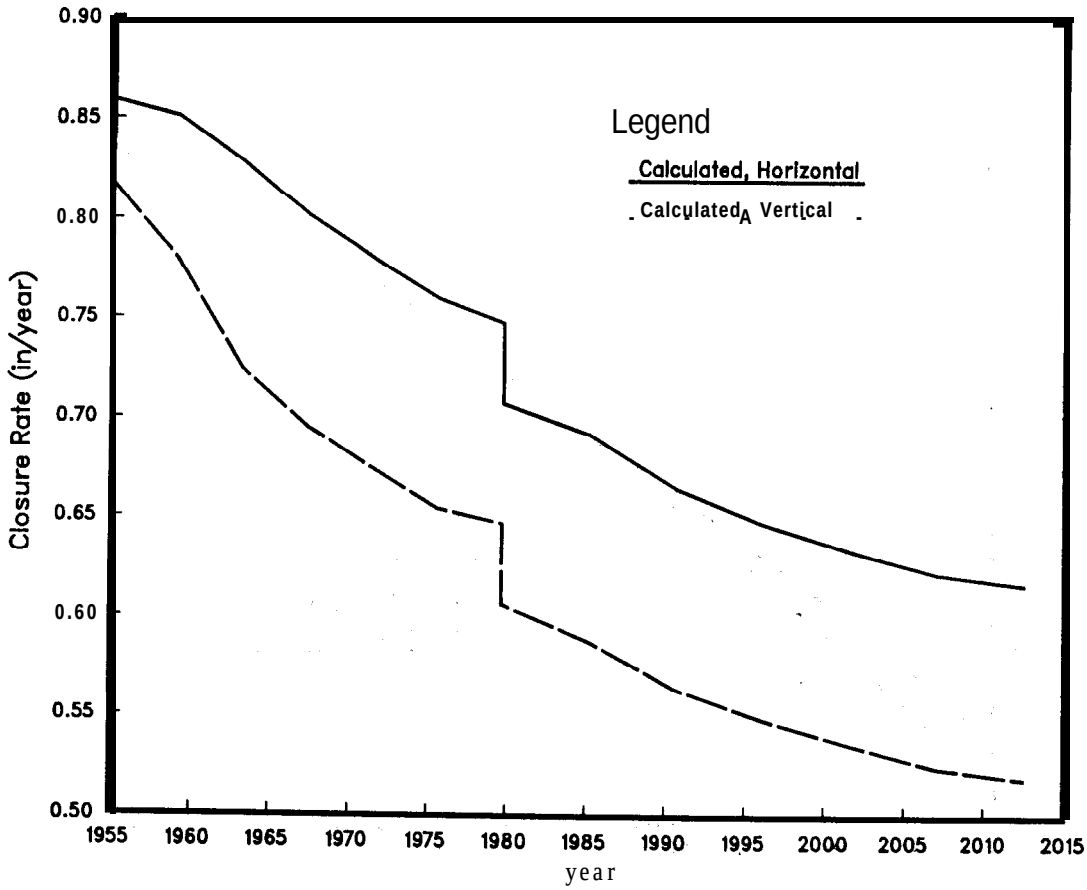

Figure 5.6: Horizontal and Vertical Closure Rate of 60 Foot Room

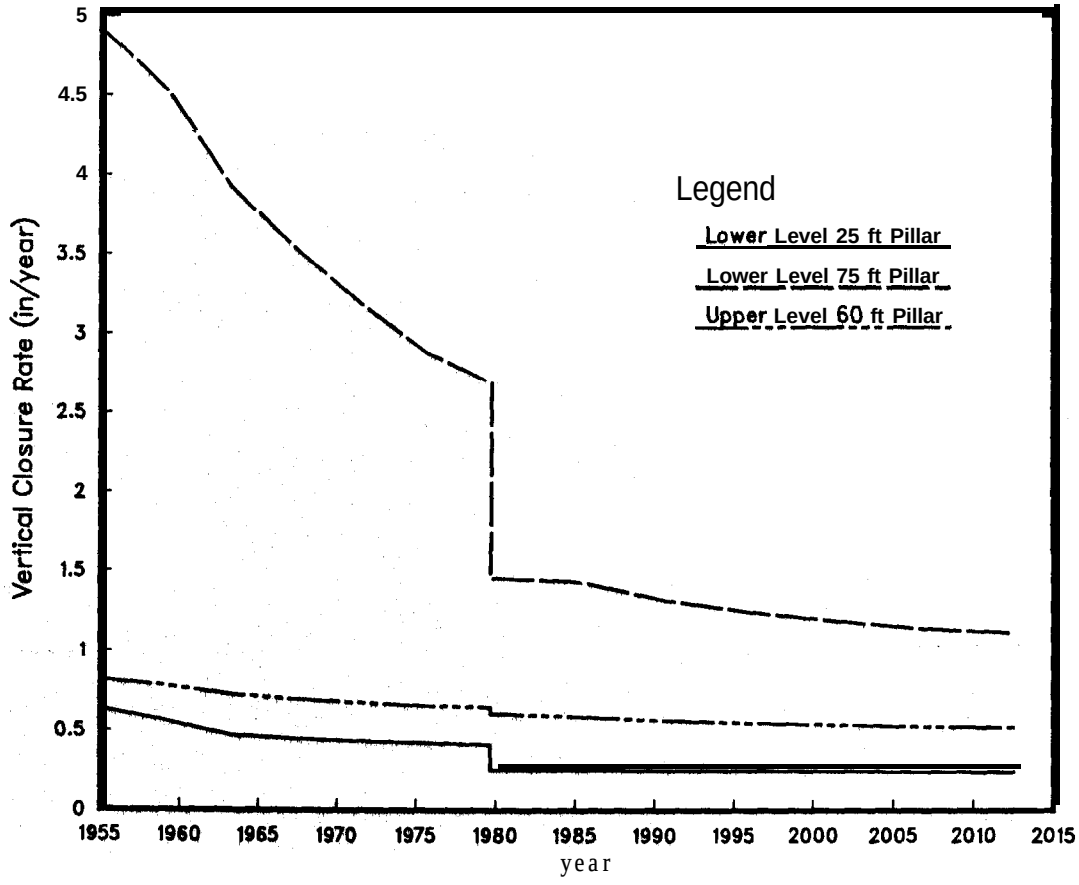

Figure 5.7: Comparison of Vertical Closures of 25 Foot Lower Level, 75 Foot Lower Level, and 60 Foot Upper Level Rooms

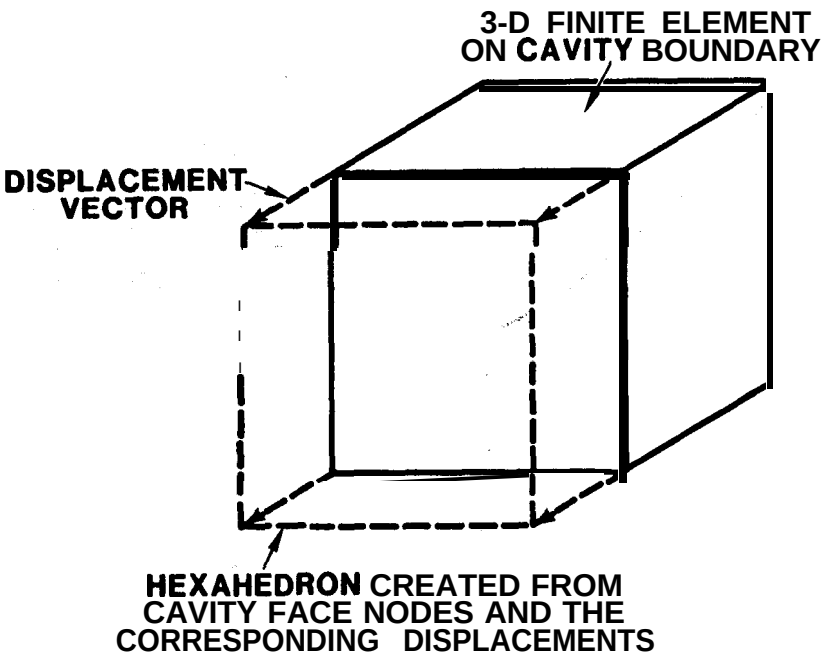

Figure 5.8: Volume Integration Using The Displacement Hexahedron Method

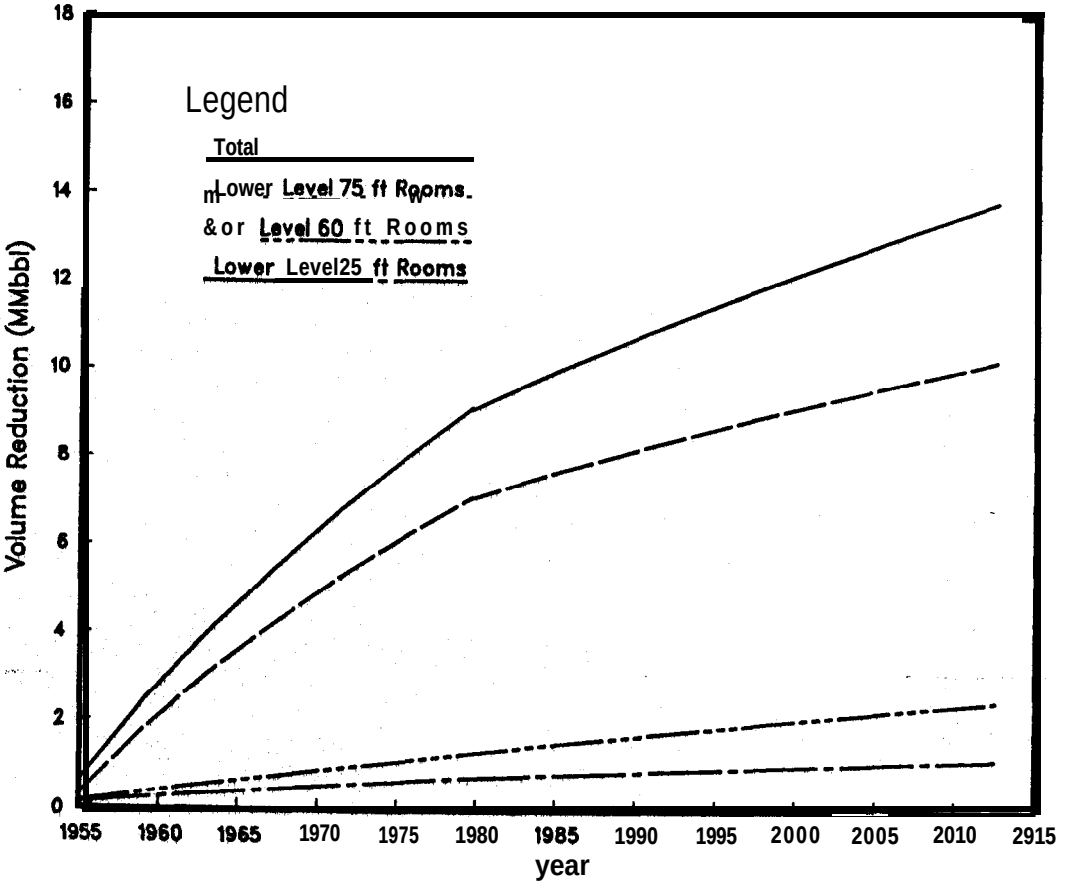

Figure 5.9: **Volume** Reduction From the Three Categories of Pillars

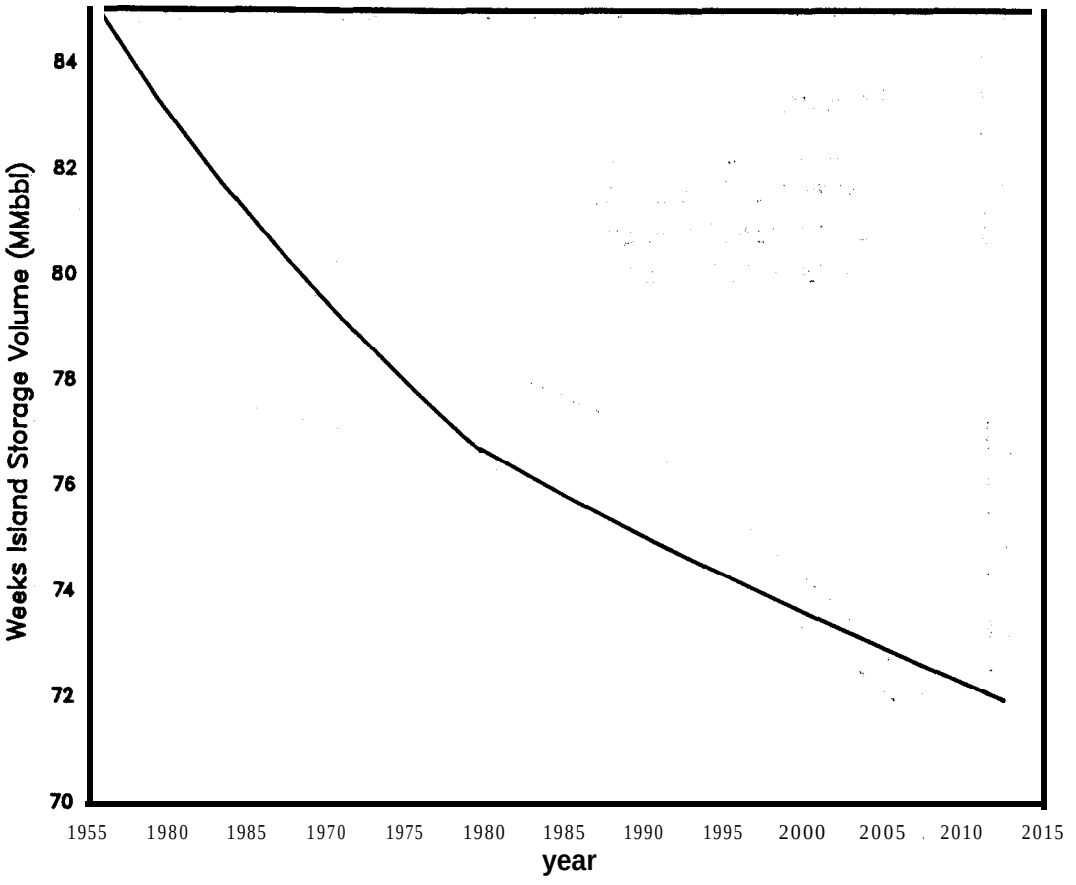

Figure 5.10: Weeks Island Storage Volume Versus Year

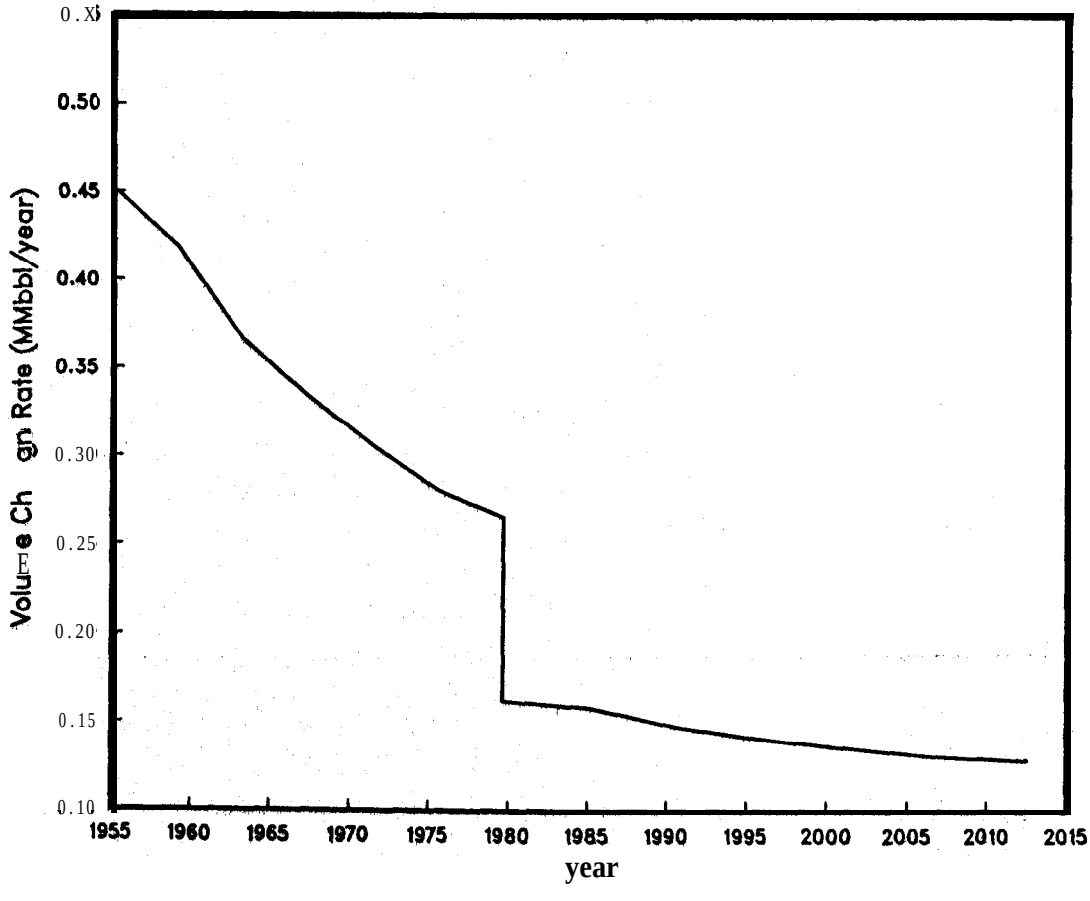

Figure 5.11: Volume Change Rate Versus Year

6. Conclusions

The storage volume reduction due to creep closure of the Weeks Island mine has been calculated using 3-D finite element models. Three models were created to represent the three pillar categories in the mine. Measured closure data for a 25 foot high room was obtained from Morton Salt and used to compute closure rates for comparison with the calculated closure rates using the 25 foot high finite element model. The comparison was relatively good which gives confidence in the models for predicting the future volume loss of the mine. Comparison of the calculated closure of the 25 foot high lower level room with the 75 foot high lower level room shows that a factor of three increase in room height results in a factor of ten increase in the closure rate. Thus, the relationship between room height and closure rate is nonlinear.

The volume change of each model at each time step was calculated using the displacement hexahedron method. The total volume change of the mine was obtained by multiplying the volume change associated with each model by the number of pillars in each category and summing over the three pillar categories. The total volume versus time curve shows that the mine lost. approximately one million barrels of storage capacity between 1977 when the mine survey was done and 1980 when oil fill began. The calculated volume change rate of the mine in 1987 was 154,000 bbl/year (3% compared with a measured rate of 165,000 bbl/year which is an approximation based (6.8% on movement of the oil/air interface. It appears from the volume versus year curve calculated in this study that the mine will deplete its excess volume in the early 1990's necessitating that several million barrels of crude oil be removed to maintain some freeboard in the mine.

REFERENCES

Acres International

Weeks Island Mine Geoteehnical Study, Contract FEA-1251-75, Acres International Inc., Buffalo, NY, November 1977.

Acres International

Additional Geotechnical Studies Strategic Petroleum Reserve (SPR), SAND86 7181, Sandia National Laboratories Contractor Report, Albuquerque, NM, December 1986.

Arguello, J. G., D. E. Munson and D. S. Preece

Preliminary ***Results*** of ***the*** Three-Dimensional Modeling ***of the WIPP Room D Excavation Sequence,*** Proceedings of 28th U. S. Symposium on Rock Mechanics, Tucson, **AZ,** June 1987

Biffle, **J. H.**

JAC - A Two-Dimensional Finite Element Computer Program for the Non-Linear Quasistatic ***Response*** of Solids With ***the Conjugate Gradient Method,*** SAND81-0998, Sandia National Laboratories, Albuquerque, NM, April 1984.

Biffle, J. H.

JAC3D Preliminary User's Manual, Internal Documentation, Sandia National Laboratories, Albuquerque, NM, 1986.

Braastetter, L. J., and D. S. Preece

Numerical Studies *of* ***Laboratory Triaxial*** Creep ***Tests,*** Proceedings of 24th U. S. Symposium on Rock Mechanics, Texas **A &** M University, College Station, TX, June 1983.

Chabannes, C, B.

Informal Transfer of Weeks Island Site ***Data,*** PB-KBB Weeks Island Site Manager, February 1987.

Fenix & Scisson Inc.

Calculation of the Storage Volume Available **in** ***the Weeks Island Mine,*** WI-22, Fenix **&** Scission Inc., Tulsa, OK, March 1977.

Hansen, F. D.

Quasi-Static ***Strength and Deformational Characteristics*** *of* ***Salt and Other Rock From the Weeks Island Mine,*** RE/SPEC Inc., Rapid City, SD, October 1977.

Hilton, P. D., S. E. Benzley and M. H. Gubbels
Structural Analysis of Weeks Island Mine/Petroleum Repository, SAND79-0595, Sandia National Laboratories, Albuquerque, NM, August 1979.

Herrmann, W. and H. S. Lauson
Analysis of Creep Data *for Various Natural Rock* Salts, SAND81-2567, Sandia National Laboratories, Albuquerque, NM, December 1981.

Krieg, R. D., C. M. Stone and S. W. Key
Comparisons of the Structural Behavior of Three Storage *Room Designs for the WIPP Project,* SAND80-1629, Sandia National Laboratories, Albuquerque, NM, 1981.

Krieg, R. D.
Implementation of Creep Equations for Metal Into a Finite Element Computer Program, Computer Methods for Nonlinear Solids and Structural Mechanics, ASME, AMD-Vol 54, pp 133-144, 1983.

Morgan, H. S., R. D. Krieg and R. V. Matalucci
Comparative Analysis of **Nine** *Structural Codes Used* in *the Second WIPP Benchmark Problem,* SAND81-1389, Sandia National Laboratories, November 1981.

Morgan, H. S., C. M. Stone and R. D. Krieg
The Use of Field Data to Evaluate and Improve Response Models for the Waste Isolation Pilot Plant (WIPP), 26th U. S. Symposium on Rock Mechanics, Rapid City, SD, June 1985.

Morgan, H. S., C. M. Stone and R. D. Krieg
An Evaluation of WIPP Structural Modeling *Capabilities Based on Comparisons With South Drift Data,* SAND85-0323, Sandia National Laboratories, Albuquerque, NM, 1986.

Morgan, H. S.
Estimate of the Time Needed for TRU Storage Rooms to Close, Sandia Memorandum to D. E. Munson, Sandia National Laboratories, Albuquerque, NM, June *2,* 1987.

Preece, D. S. and W. R. Wawersik
Leached Salt Cavern Design Using a Fracture Criterion for Rock Salt, Proceedings of the 25th U. S. Symposium on Rock Mechanics, Northwestern University, Evanston, Illinois, June 1984.

Preece, D. S. and R. D. Krieg
Finite Element Study of Working Level Separation at the Weeks Island Salt Dome, SAND84-1021, Sandia National Laboratories, Albuquerque, NM, July 1984.

Preece, D. S. and H. J. Sutherland
Physical and Numerical Simulations of Fluid-Filled Cavities in *a Creeping Material,* SAND86-0694, Sandia National Laboratories, Albuquerque, NM, May 1986.

Stone, C. M., R. D. Krieg and Z. E. Beisinger
SANCHO - A Finite Element Computer Program for the Quasistatic, Large Deformation, Inelastic Response of Two-Dimensional Solids, SAND84-2618, Sandia National Laboratories, Albuquerque, NM, April 1985.

Wawersik, W. R., and D. H. Zeuch
Creep and Creep Modeling of Three Domal Salts - A Comprehensive Update, SAND84-0568, Sandia National Laboratories, Albuquerque, NM, May 1984.

Distribution:

US DOE SPR PMO (10)
900 Commerce Road East
New Orleans, LA 70123
E. E. Chapple, PR-63 (5)
L. J. Rousseau, PR-63 (1)
J. W. Smollen, PR-63 (2)
TDCS (2)

US Department of Energy (1)
Strategic Petroleum Reserve
1000 Independence Avenue SW
Washington, DC 20585
D. Smith

US Department of Energy (1)
Oak Ridge Operations Office
P. 0. Box E
Oak Ridge, TN 37831
J. Milloway

Acres International Corporation (3)
Suite 1000 Liberty Building
424 Main Street
Buffalo, NY 14202-3592
Bill Lamb
Stewart Thompson
Tom Magorian

Aerospace Corporation (2)
800 Commerce Road West, Suite 300
New Orleans, LA 70123
R. Merkle

PB/KBB (4)
850 South Clearview Parkway
New Orleans, LA 70123
H. Lombard (4)

PB/KBB (2)
Weeks Island
P. 0. Box 434
New Iberia, LA 70560
C. Chabannes (2)

Boeing Petroleum Services (5)
850 South Clearview Parkway
New Orleans, LA 70123
J. Schmedeman (4)
K. Mills

Walk-Haydel & Associates, Inc. (3)
600 Carondelet St.
New Orleans, LA 70130
Cary Trochesset
John Rabai
J.Mayes

Dr. S. E. Benzley
Civil Engineering Dept. 368CB
Brigham Young University
Provo, Utah 84602

Dr. C. H. Conley
School of Civil and Environmental Engineering
Hollister Hall
Cornell University
Ithaca, NY 14853

Sandia Internal:

1510 J. W. Nunziato
1520 C. W. Peterson
1521 R. D. Krieg
1521 H. S. Morgan
1521 D. S. Preece (20)
1530 L. W. Davison
1550 R. C. Maydew
3141-1 S. A. Landenberger (5)
3154-4 C. Dalin, For: DOE/TIC (28)
3151 W. L. Garner (3)
6000 D. L. Hartly
6200 V. L. Dugan
6230 W. C. Luth
6232 W. R. Wawersik
6232 D. H. Zeuch
6250 B. W. Marshall
6257 J. K. Linn (10)
6257 J. L. Todd
6257 J. T. Neal
6332 L. D. Tyler
6332 J. G. Arguello
8024 P. W. Dean